Journal of Micromechatronics, Vol. 00, No. 0, pp. 1–13 (2004)

Also available online - www.vsppub.com

Development of a peristaltic pump in printed circuit boards

NAM-TRUNG NGUYEN * and XIAOYANG HUANG

School of Mechanical and Production Engineering, Nanyang Technological University, Nanyang Avenue, Singapore 639798, Republic of Singapore

Abstract—This paper presents the development of a peristaltic pump based on the printed circuit board (PCB) technique. The pump was fabricated by using PCB as the substrate material and standard PCB techniques (copper etching, soldering). The paper describes in details the development process including the numerical simulation of the pump effect, the investigation of the piezoelectric actuator, the fabrication and the characterization. A maximum flow rate of 3 ml/min can be achieved with a single peristaltic pump. One of the applications of the peristaltic pump is a self-cooling printed circuit board (SC-PCB). The SC-PCB consists of three peristaltic pumps, a channel system for fluid circulation, and a heat sink. The SC-PCB shows great potentials in thermal management of electronic devices.

Keywords: Printed circuit board; micropumps; piezoelectric actuators; active cooling.

1. INTRODUCTION

Microfluidics has been established as a new engineering discipline with a huge scientific and commercial potential. In the last decade, research on microfluidic devices and fluidic phenomena on a micro-scale becomes a strategic topic of the international research community. A number of fluidic components have been realized in silicon technology. The most common components are micropumps, valves, flow sensors, separators and mixers [1–5].

Despite the research effort and the promisingly huge market, microfluidic systems still can not establish widely in the commercial application. One of the reasons is the relatively high development and fabrication cost of silicon based microfluidic systems.

In order to make the cost of a microfluidic system acceptable, alternative fabrication methods like plastic molding and hot embossing can be used. Our approach

*To whom correspondence should be addressed. E-mail: mntnguyen@ntu.edu.sg

Table 1.
Typical parameters of MEMS, PCB and microfluidic devices

Parameters	MEMS	PCB	Microfluidics
Resolution	5 μm	100 μm/min	50 μm–10 mm
Clean room class	10^2–10^3	10^3–10^4	Typically 10^3
Electronic compatibility	Typically 4 metal layers	4–20 metal layers	Typically 1 metal layer
Bonding techniques	Anodic, diffusion, adhesive	Eutectic, lamination (adhesive)	Anodic, diffusion, adhesive

used PCB as a substrate for electronic components as well as fluidic elements. Table 1 compares some common parameters of MEMS technology, PCB-technology and those required by microfluidic systems. The comparison shows that PCB can be the solution for systems with no critically small structures.

With higher integration density and higher operating frequency, integrated circuits generate more heat. The thermal management becomes more and more important as well as more difficult for designers of electronic devices. Using microfluidic devices for active cooling, most of the reported works followed the on-chip approach. Channels for liquid flow [6] or jet nozzle [7] are integrated into the silicon chip. For the near future, the on-chip approach is not mature for real applications because of the lack of a practical solution for the chip packaging, for the fluidic interconnection and fluid flow generation. With more self-cooling chips in an electronic device, this problem will become more crucial.

As an application of the PCB technique, we demonstrate in this paper the on-board active cooling approach. One or more PCB-pumps and fluid channels are integrated into the PCB. The design of the fluidic interconnection and the heat sink is than on the board level, which is simpler to handle.

2. OPERATION PRINCIPLE AND NUMERICAL SIMULATION

In recent years, numerous micro-pumps with a wide spectrum of operation principles were reported. Because the PCB technique is limited for simple fluidic structures, we focused on valveless principles. Valveless pumps do not require check valves, and are divided into the following categories:

- Peristaltic pumps, which can have a maximum flow rate of 100 μl/min, as reported in Ref. [8] for water.
- Diffuser/nozzle- and valvular conduits pumps, which can generate a maximum flow rate of 2000–3000 μl/min water [9, 10].
- Ultrasonic pumps, which induce acoustically a flow rate on the order of 10 μl/min [11, 12].

- Electro-osmotic and electrophoresis pumps, which can move liquids with a velocity of less than 1 mm/s. Depending on the capillary diameter and the applied voltage, a flow rate of several hundred nl/min can be achieved [13].

The first category is simple and does not required special technologies. Hence, we used the peristaltic pump for the integration on the PCB.

Peristaltic pumps synchronize several piezo-discs and the corresponding pump chamber in a wave-like motion. This peristaltic motion transports the fluid in the direction opposite to the wave motion. Macroscopic peristaltic pumps generate the wave-like motion by a wheel with roles along the circumference. The roles press on a flexible silicon rubber tube and cause the wave-like motion when the wheel rotates. The micromachine peristaltic pump reported in Ref. [8] used active valves at the outlet and the inlet, the signaling scheme did not describe a true wave-like motion.

A minimum number of 3 piezo-discs is required for a wave-like motion. Figure 1 illustrates the signaling scheme for the 3 piezo-discs in our design. The piezo-discs were actuated by square-wave signals. The second and the third signals have a phase shift of 90° and 180° to the first signal. In Fig. 1, the wave motion goes from left to right, while the fluid flows from right to left.

When the first signal is switched to high level, the first disc sucks the fluid from the second disc into the first pump chamber while the third disc is closed and pushes the fluid to the second chamber (stage 1, Fig. 1b). With a 90° phase shift, the second

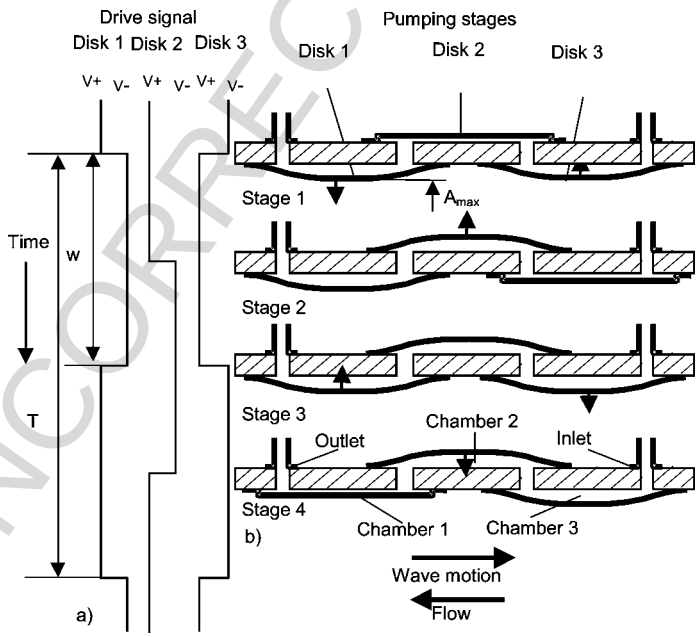

Figure 1. Operation principle of the peristaltic pump. (a) Signaling scheme (V+ and V− indicate the high and low signal levels). (b) The corresponding pumping stages.

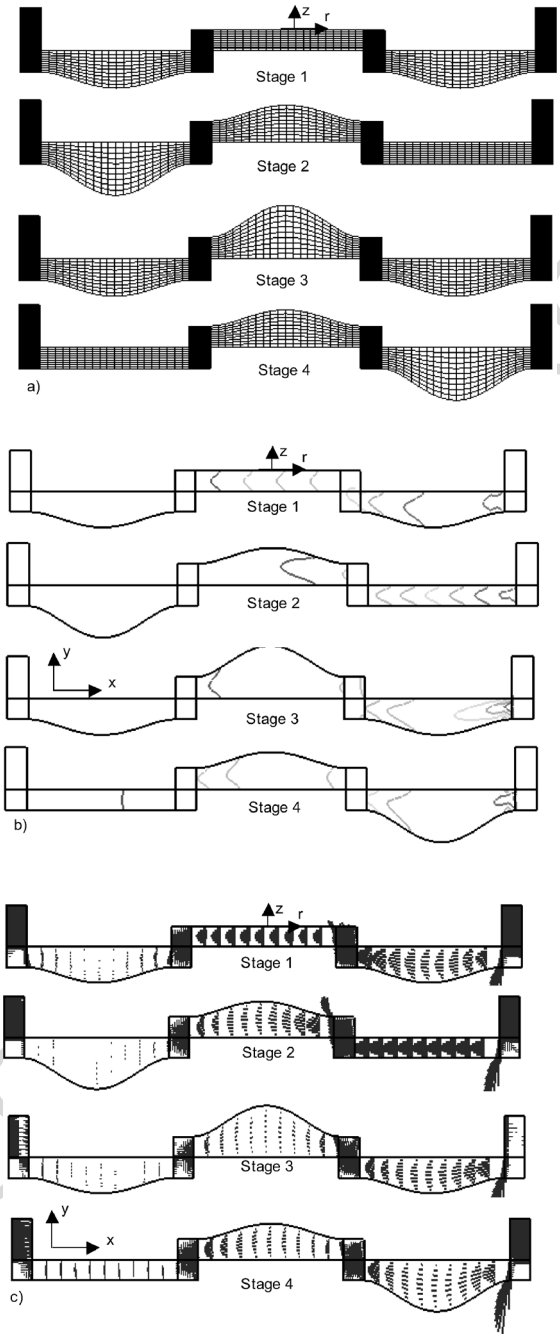

Figure 2. Results of the velocity field in a simplified model for the peristaltic pump (water, 100 Hz pump frequency, 40 μm maximum deflection, the y-axis in this figure is scaled up 50 times). (a) The grid model; (b) the pressure distribution; (c) the velocity field.

disc is opened and sucks the fluid from the third chamber into the second chamber. Due to its inertia the fluid continues to flow to the outlet. In the third stage, disc 1 is closed and pushes the fluid to the outlet. While the second chamber is still opened, disc 3 sucks the fluid from the inlet into the third chamber. In the last stage of the pumping period, disc 2 pushes the fluid out of the second chamber. The fluid is pushed through the first chamber to the outlet.

We used a simplified model of the pump. The numerical model consists of three pump chambers with three actuating walls. The middle chamber is on the same side with the inlet and outlet. The moving wall condition is used for all three chambers. The moving grids are calculated for each pump chamber in every time steps using a user routine written in FORTRAN. For simplification, the membrane deflection dz assumed the Timoshenko's deflection model for thin circular plates [14]:

$$dz(r,t) = A_0(t)\left[1 - \left(\frac{r}{R}\right)^2\right]^2, \tag{1}$$

where r is the radial coordinate and A_0 the time-dependent deflection of the center of the piezo-disc taken from experiments described in the next section. For a square wave drive voltage with a time period T, the deflection $A_0(t)$ can be approximated using Fourier series as:

$$A_0(t) = \frac{C_0}{2} + \sum_{n=1}^{\infty}\left(C_n \cos\frac{2n\pi t}{T}\right) \quad \text{with } n = 1, 2, 3\ldots \tag{2}$$

with the coefficients

$$C_0 = 2A_{\max} \cdot \frac{w}{T}, \tag{3}$$

$$C_n = \frac{2A_{\max}\sin\left(\dfrac{n\pi w}{T}\right)}{n\pi}, \tag{4}$$

where $A_{\max}$ is the membrane deflection when a voltage is applied and w is the corresponding pulse width (Fig. 1).

Figure 2a presents the grid model of the peristaltic pump in each pumping stage. Results of the pressure field and the corresponding velocity field inside the pump are shown in Fig. 2b and Fig. 2c, respectively. The four stages correspond to the stages illustrated in Fig. 1. The results show clearly the left-to-right wave motion of the actuators, which causes a fluid flow in opposite direction: from right to left.

3. FABRICATION

3.1. Piezoelectric actuator disc

In order to keep the design simple, commercially available piezo discs are selected as actuators. These piezo-discs are used as buzzers in electronic equipments.

The piezo-disc consists of a piezoelectric ceramic layer glued on a brass disc. Our pump design uses the brass disc as the pump membrane. The brass disc has a diameter of 15 mm and a thickness of 95 μm. The piezoelectric layer has a diameter of 12 mm and a thickness of 175 μm. With a maximum drive voltage of 200 V, the maximum electrical field strength is 1.1 kV/mm, which is lower than the break down field of most common piezoelectric materials (more than 2 kV/mm).

In this paper, we define the top electrode of the piezo-disc as the voltage terminal and the brass disc as the ground terminal. The square wave signal at the voltage terminal has the high potential level $V+$ and a low potential $V-$.

The electric field applied on the piezoelectric layer induces an expanding strain in the disc perpendicular to the electric field and a contracting strain in the direction of

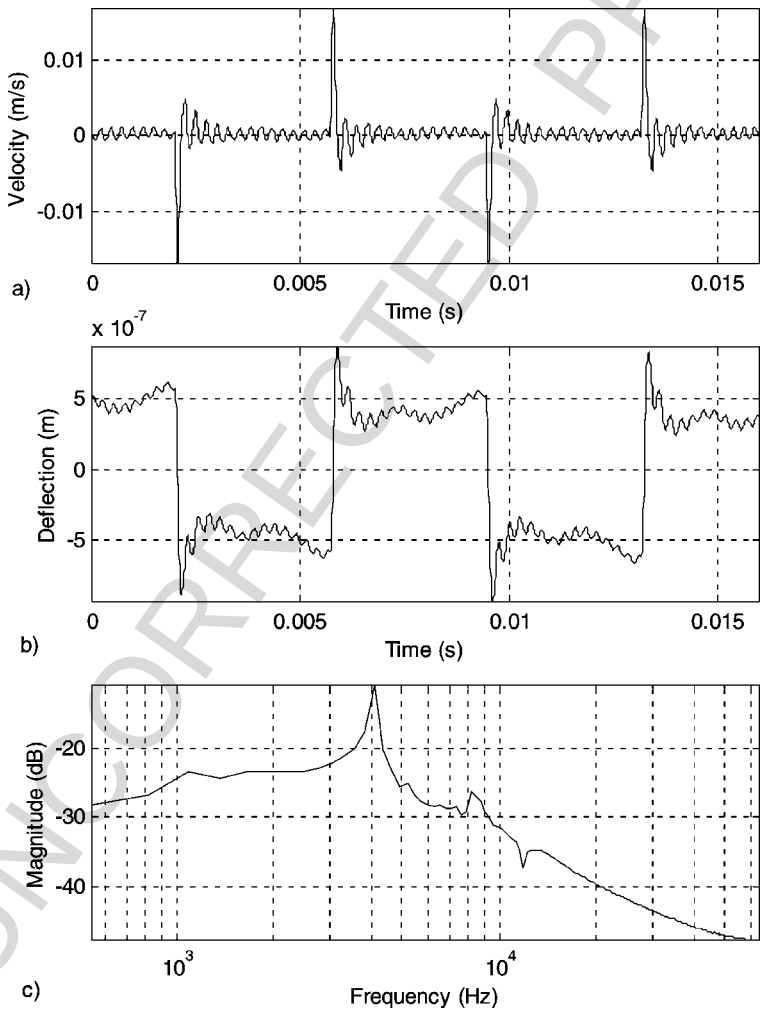

Figure 3. Results of vibration measurement ($V = \pm 30$ V, pump chamber filled with air). (a) Velocity, (b) displacement, (c) transfer function of the piezo-disc.

the disc thickness (assuming that the piezoelectric coefficient d_{31} is negative and d_{33} is positive). Since the piezoelectric layer is tightly glued to the brass disc, there are reacting forces from the brass disc opposing the expansion of the piezoelectric layer. This motional restriction causes the deflection of the disc. Our work focuses on the experimental characterization of the time-dependent bending of the piezo-disc.

The piezo disc was characterized by the Polytech laser vibrometer. The piezo disc of the pump shown in Fig. 1 was investigated. The piezo-disc was soldered to the PCB. Figure 3 shows the dynamic characteristics of the center of the piezo-disc. Since the vibrometer only measured the vibration velocity (Fig. 3a), the disc deflection was calculated based on the velocity and time data. Using this measurement system, the absolute deflection could not be measured because of the unknown initial condition. The results of the disc deflection were, therefore, corrected by a first-order fitting function, which eliminates the offset and centers the deflection on zero (Fig. 3b). Based on the deflection data and the excitation signal, the transfer function of the disc was calculated (Fig. 3c). The transfer function identified the piezo-disc as a typical second-order system with a resonant frequency of about 4 kHz.

With the technique described above, the disc deflection at a given voltage can be measured (Fig. 3b). The disc deflection versus the drive voltage is illustrated in Fig. 4. In Fig. 4, the circles are measurementf points, the line is the polynomial fitting function. The deflection-voltage characteristics have a typical quadratic behavior.

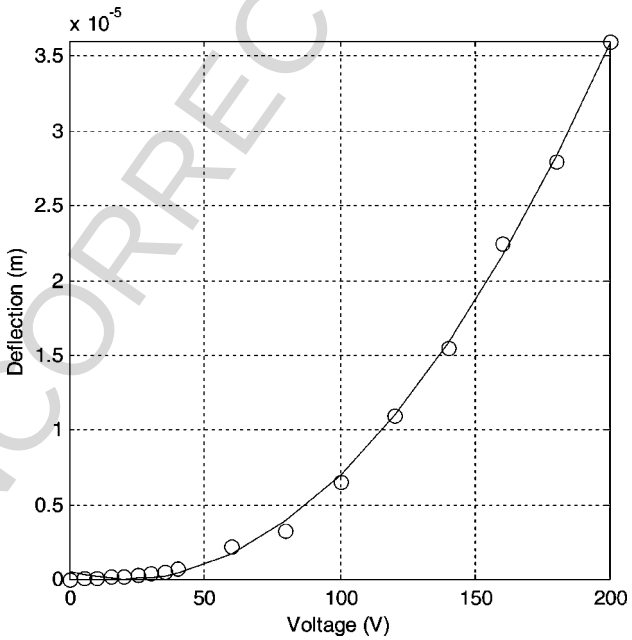

Figure 4. The deflection as function of voltage (solid line is the fitting function $dz = 0.0011 \cdot V^2 + 0.0477 \cdot V + 0.5495$).

3.2. Device fabrication

Figure 5a presents the fabrication of the single peristaltic pump. The pump chamber was etched in the copper layer and has a height equal the thickness of the copper layer (about 40 μm for a standard two-sided PCB). The inlet, the outlet, and the connecting orifices between the pump chambers were drilled in the PCB substrate. The inlet and outlet tubes were plugged into the orifices. Subsequently, the three

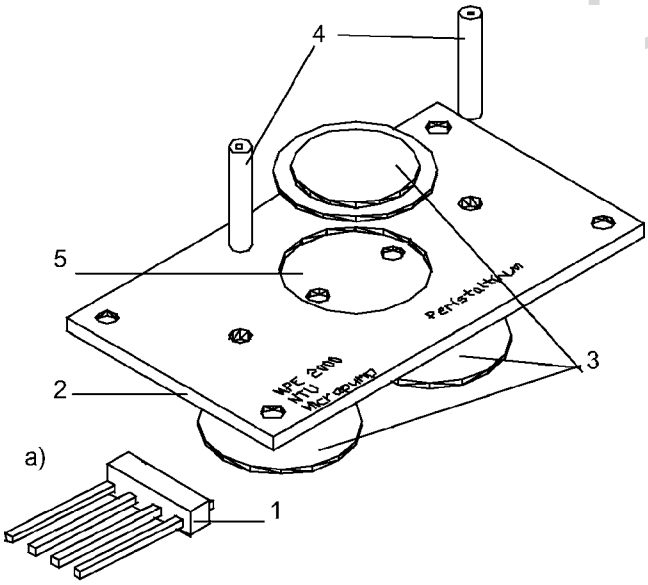

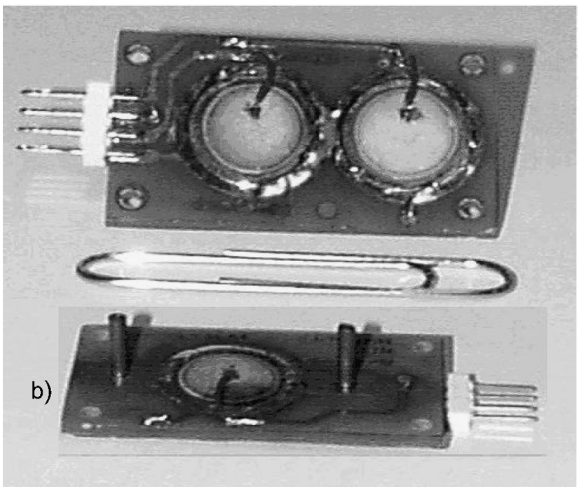

Figure 5. The peristaltic pump. (1) Header for electric interconnection, (2) PCB, (3) piezo discs, (4) inlet/outlet tubes, (5) pump chamber etched in the copper layer.

piezo-discs were soldered directly onto the copper layer. Fig. 5b shows the finished peristaltic PCB pump.

3.3. Drive circuitry

Figure 6 illustrates the circuitry implementing the signaling scheme described above. The universal timer LM555 generates the square wave signal for disc 1. A simple phase shifter based on 2 logical NANDs and a RC-bridge shifts the second signal. A logical negator implements the third signal, which is shifted 180° from the first signal. The three signals are used for switching 3 electromechanical relays. The piezo discs are switched between two voltage levels: $V+$ and $V-$. These two drive voltages are supplied from an external high voltage source. For high-frequency switching and avoiding noises, solid state relays with opto-electronic coupling can be used instead of electromechanical relays.

4. EXPERIMENTAL CHARACTERIZATION

The pump was tested with water. We used a simple setup described in Fig. 7. The flow rate was calculated from the velocity of the water-air interface at the pump outlet and the tube diameter. The velocity was measured manually by a ruler and a stopwatch. In the experiments, the lower voltage level was kept at ground ($V- = 0$ V), while the piezo-discs were driven by the high voltage level $V+$.

Figure 8 shows the measured flow rate *versus* the drive frequency. For frequencies less than 50 Hz, the flow rate increases proportionally with the frequency. The flow rate reaches its maximum at 50 Hz. The flow rate decreases at higher frequencies because of the large inertia of the fluid in the pump. If the flow rate is controlled by the drive frequency, the operation range lies between 0 and 50 Hz.

Figure 9 illustrates the flow rate versus the drive voltage $V+$. The circles are measured results. The line is the parabolic fitting curve. A relatively high flow rate of 3 ml/min can be achieved with 140 V. A number of this pump working in parallel is able to generate a flow rate for active cooling applications described in the next section.

Figure 10 illustrates the flow rate vs. membrane deflection characteristics. The data was taken from the results shown in Fig. 9, the membrane displacements were calculated by the fitting function of Fig. 4.

5. CONCLUSIONS

A simple and low-cost peristaltic pump has been designed and developed based on the PCB-technique. The results have shown that the use of PCB as substrate material for microfluidic systems is possible and economical. Low cost, fast development time and flexible production can be achieved. The PCB micropumps can achieve a maximum flow rate of 3 ml/min. Smaller flow rate with precise control can be designed with smaller piezo-discs. The maximum drive voltage and frequency

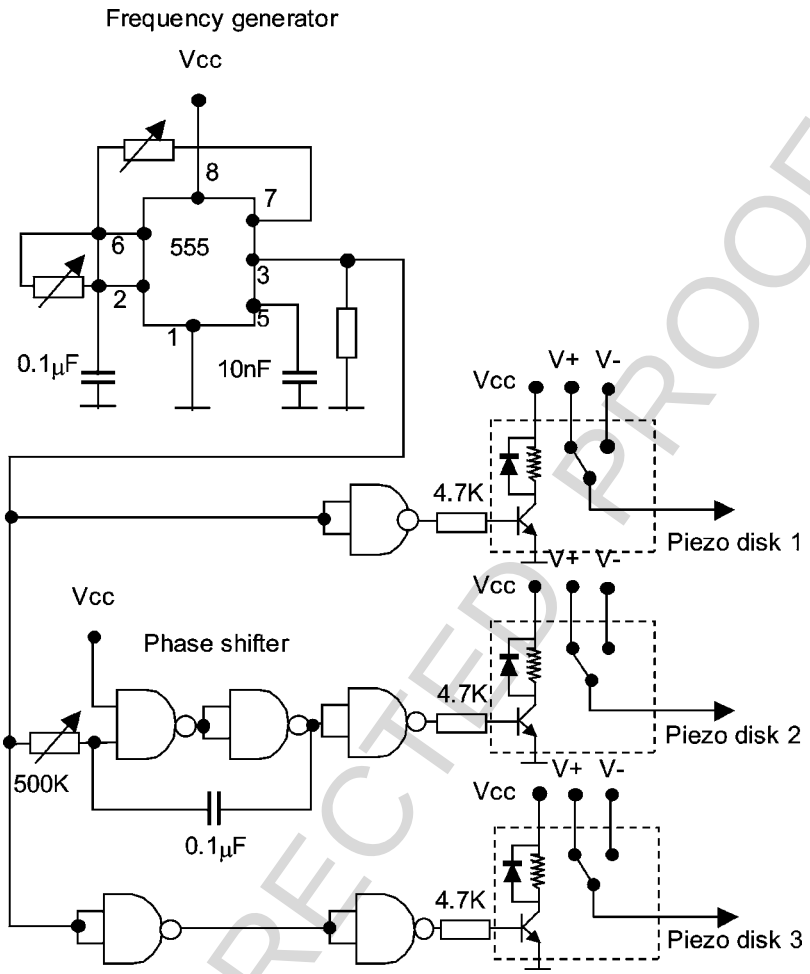

Figure 6. Scheme of the control circuitry for the peristaltic pump (dashed boxes are commercial relays).

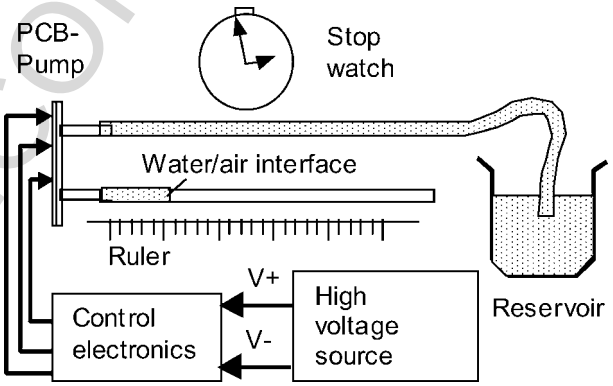

Figure 7. Experimental setup.

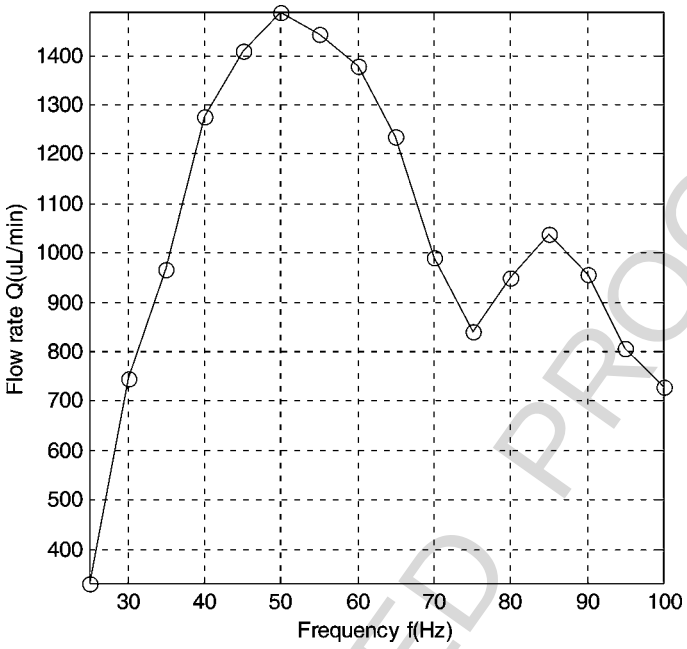

Figure 8. Flow rate *versus* drive frequency ($V- = 0$; $V+ = 100$ V).

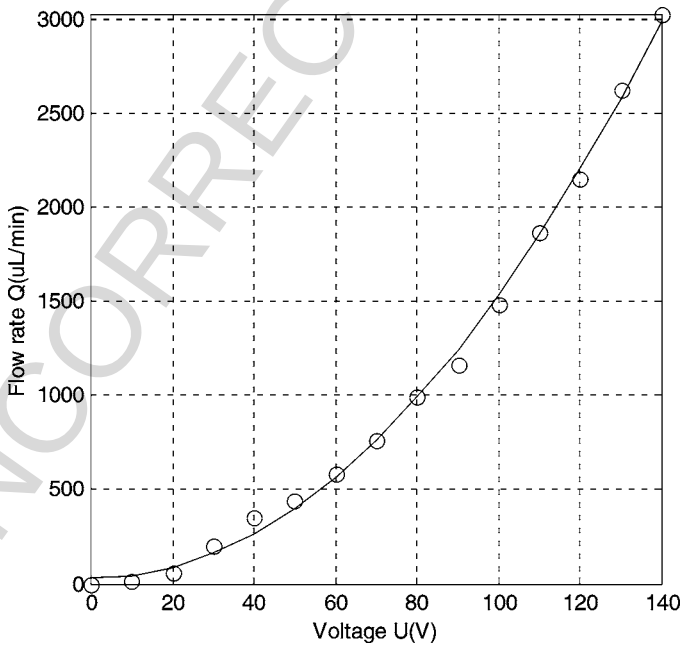

Figure 9. Flow rate *versus* drive voltage ($V- = 0$, $f = 50$ Hz).

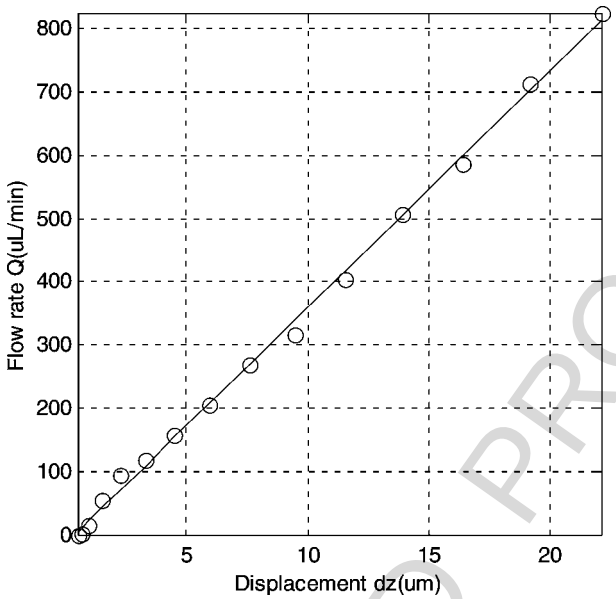

Figure 10. Flow rate *versus* displacement of the pump membrane (data from measurements presented in Figs 5 and 10).

of such pumps are about 150 V and 100 Hz, respectively. Higher voltages or frequencies may destroy the actuator because of the high electric and thermal load.

Further investigation with PCB based on ceramic substrate and thick film technology promises smaller and more complex devices with self-cooling capabilities. Traditional techniques like soldering, electroplating, multi-layer lamination and drilling can be used in the PCB fluidic system.

REFERENCES

1. S. Shoji and M. Esashi, Microflow devices and systems, *J. Micromech. Microeng*. **4**, 157–171 (1994).
2. P. Gravesen, J. Branebjerg and O. S. Jensen, Microfluidics — a review, *J. Micromech. Microeng*. **3**, 168–182 (1993).
3. M. Elwenspoek, T. S. Lammerink, R. Miyake and J. H. J. Fluitman, Towards integrated microliquid handling system, *J. Micromech. Microeng*. **4**, 227–245 (1994).
4. G. Stemme, Micro fluid sensors and actuators, in: *Proceedings of the 6th International Symposium on Micro Machine and Human Science*, pp. 45–52.
5. D. A. Patterson and J. L. Hennessy, Cost and trends in cost, in: *Computer Architecture a Quantitative Approach, Chapter 1.4*, pp. 18–28. Morgan Kaufmann Publishers, San Francisco, CA (1997).
6. L. Jiang, M. Wong and Y. Zohar, Phase change in micro channel heat sinks with integrated temperature sensors, *J. Micromech. Syst*. **8**, 358–365 (1999).
7. S. Wu, J. Mai, Y. C. Tai and C. M. Ho, Micro heat exchanger by using MEMS impinging jets, in: *Proceedings of the 12th Annual IEEE International MEMS '99 Conference*, Orlando, FL (1999).

8. J. G. Smits, Piezoelectric micropump with three valves working peristaltically, *Sensors Actuators A* **40**, 203–206 (1990).
9. A. Olsson, Valveless diffuser micropumps, PhD Thesis, Royal Institue of Technology, Sweden (1998).
10. F. K. Forster, L. Bardell, M. A. Afromowitz, N. R. Sharma and A. Blanchard, Design, fabrication and testing of fixed-valve micropumps, *Proc. ASME Fluid. Eng. Div*. **234**, 39–44 (1995).
11. N. T. Nguyen and R. M. White, Design and optimization of an ultrasonic flexural plate wave micropump using numerical simulation, *Sensors Actuators A* **77**, 229–236 (1999).
12. N. T. Nguyen, A. H. Meng, J. Black and R. M. White, Integrated flow sensor for in situ measurement and control of acoustic streaming in flexural plate wave micro pumps, *Sensors Actuators A* **79**, 115–121 (1999).
13. A. E. Herr, J. I. Molho, T. W. Kenny, J. G. Santiago, M. G. Mungal and M. G. Garguilo, Variation of capillary wall potential in electrokinetic flow, *Proc. Tranduc*. **99**, 710–713.
14. S. P. Timoshenko and S. Woinosky-Krieger (Eds), *Theory of Plates and Shells, Volume 3*. McGraw-Hill, New York, NY (1959).

ABOUT THE AUTHORS

Nam-Trung Nguyen was born in Hanoi, Vietnam, in 1970. He received the Dipl.-Ing. and Dr.-Ing. Degrees in Electronic Engineering from Chemnitz University of Technology (Chemnitz, Germany), in 1993 and 1997, respectively. In 1998, he worked as a postdoctoral researcher in the Berkeley Sensor and Actuator Center (EECS, University of California at Berkeley, CA, USA). He is currently an assistant professor with the School of Mechanical and Production Engineering of the Nanyang Technological University in Singapore. Dr. Nguyen published several journal papers on microfluidics. He is also the author and co-author of five books in German, English and Vietnamese.

Xiaoyang Huang received his BSc in physics in 1982 from Nanjing University (Nanjing, China) and PhD in acoustics in 1989 from Cambridge University (Cambridge, UK). Currently he is an Associate Professor at the School of Mechanics and Production Engineering, Nanyang Technological University (Singapore). His research interest has been in acoustics, unsteady flow control, heat transfer, and now in micro-fluidic systems.